WFIRST Technical Report
Doc #: WFIRST-STScI-TR1606
Rev: A
Date: October 27, 2016

On the Effects of Extended-Source Morphology on Emission-Line Redshift Accuracy

R. E. Ryan Jr., S. Casertano, & N. Pirzkal

Abstract

We discuss the effects of emission-line regions distributed asymmetrically in extended galaxies on redshift estimates. Using published estimates for the distance distribution of line-emitting regions, we present a Monte Carlo simulation and establish that the redshift uncertainty is typically $\sigma_z/(1+z) \sim 0.0007$. We discuss several options to mitigate this uncertainty, most of which require data taken in multiple orients.

1 Introduction

The *Wide-Field Infrared Survey Telescope* (WFIRST) is a NASA-planned observatory with a variety of data and scientific goals. The High-Latitude Survey is one key project that will obtain imaging and spectroscopy over ~ 2200 deg^2 to address key issues involving dark energy and galaxy evolution. This program will require fairly accurate redshifts; the WFIRST-AFTA Final Report requires a fractional uncertainty in $(1+z)$ of $\sigma_z/(1+z) \leq 0.001 - 0.005$ at $0 \leq z \leq 3$ (Spergel *et al.* 2015). To this end, the spectroscopic survey will be conducted with a single grism element roughly covering $\sim 1 - 2$ μm with a resolution of ~ 10 Å pix^{-1}, although many aspects of this grism are currently under active discussion.

However observations of galaxies at $z \lesssim 1$ with prominent emission lines (EW$_{\rm rest} \gtrsim 100$ Å) in one of Hα, [O II], and/or [O III] often exhibit significant spectral diversity: the spatial distribution of the line emission differs from that of the continuum flux (*e.g.* Nelson *et al.* 2012). Therefore, if the position of the line emission is estimated from the broadband images, this will result in a random error on redshift as determined from the emission line. This issue may be exacerbated at $z \sim 1$, where a significant fraction of galaxies are clumpy and star-forming (*e.g.* Ravindranath *et al.* 2006; Law *et al.* 2012; Guo *et al.* 2015), and some of the clumps have been identified as emission-line regions (ELRs, Pirzkal *et al.* 2013). Ignoring this effect leads to erroneously assigning the observer-frame wavelengths due to offsets in line- and continuum-emission, which will ultimately introduce a non-statistical random uncertainty in the spectroscopic redshifts. The primary goal of this Technical Report is to establish the *order-of-magnitude* for this additional redshift uncertainty.

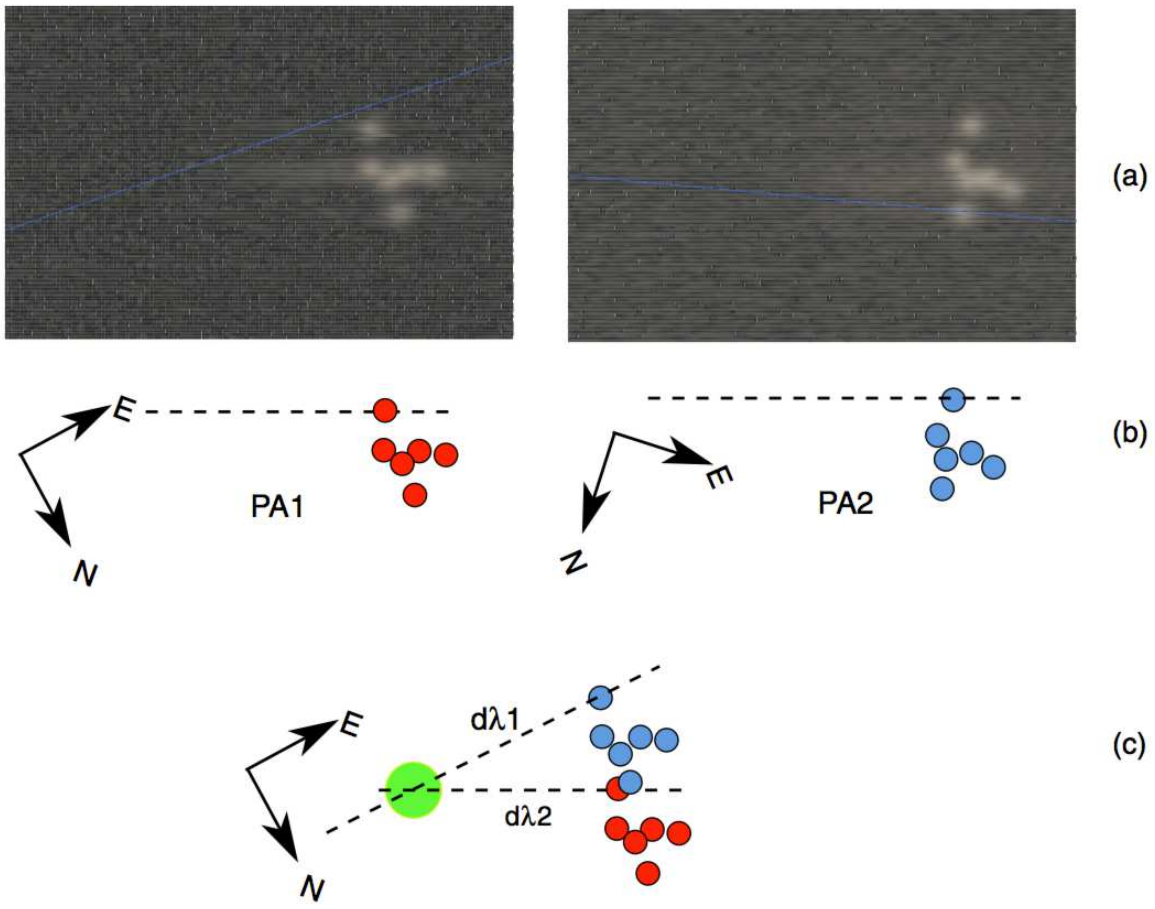

Figure 1: Emission-line region triangulation (this figure is taken from Straughn *et al.* 2008). Top panel: dispersed images at two different position angles. Middle panel: schematic of the emission lines (the dashed line indicates the dispersion direction). Bottom panel: remapping of the two images onto sky positions. This figure highlights clumpiness of the line emission and the triangulation method (discussed in § 3).

We organize this Technical Report as follows: we describe our emission-line galaxy model in § 2, discuss several crude ideas for mitigation techniques in § 3, and give concluding remarks in § 4.

2 Emission-Line Regions: Extended Sources

Pirzkal *et al.* (2013) show that the galactocentric distance distribution of ELRs, scaled to the half-light radius of the host galaxy, is roughly an exponential distribution (see Figure 2). Based on the Kolmogorov-Smirnov test, they conclude that the distribution of galaxies with 1 ELR or >1 ELR are consistent, therefore we average the two distributions (these distributions are shown in Figure 2 as histograms with the different hatching patterns). By fitting the averaged distribution, we find:

$$n(x) \propto \exp(-1.82\,x), \tag{1}$$

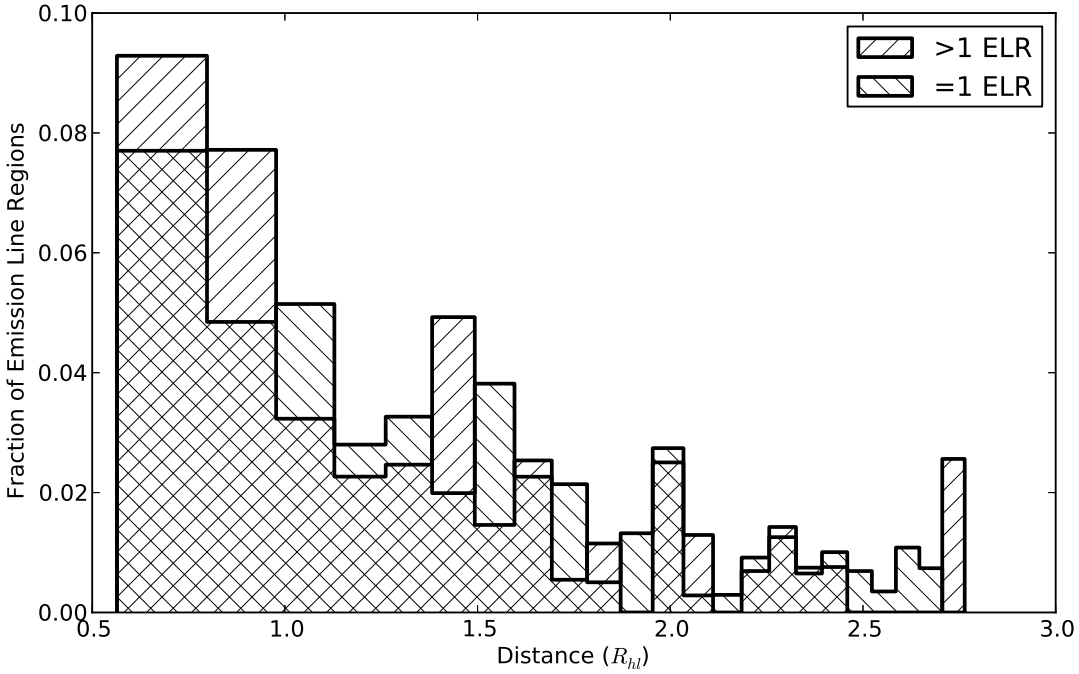

Figure 2: Distribution of galactocentric distances of emission-line regions (ELRs) in units of the half-light radius (R_{hl}) of the host galaxies irrespective of the line species (this figure is reproduced here from Pirzkal *et al.* 2013). The various hatched histograms show the distribution for galaxies with a single ELR (negative-slope hatches) and multiple ELRs (positive-slope hatches). Pirzkal *et al.* (2013) argue these two distributions are likely drawn from the same parent distribution, and so we average these together to establish the characteristic scale of an exponential distribution given in Equation 1.

where $x = r/R_{hl}$, with r is the galactocentric distance and R_{hl} is the half-light radius.

Nagy *et al.* (2011) show that the galaxy half-light radius for star-forming galaxies at $1.5 \lesssim z \lesssim 2.0$ only weakly depends on the galaxy stellar mass (their Table 1), which is consistent with what is seen in the Sloan Digital Sky Survey (SDSS) at low redshift. Therefore we average the Nagy *et al.* (2011) results over stellar mass (*i.e.* the second row of their Table 1) and find that $R_{hl} = 1.9 \pm 0.4$ kpc, which is consistent with other reports (*e.g.* Ferguson *et al.* 2004; Mosleh *et al.* 2012).

To simulate the effects of extended-emission line sources, we perform a simple Monte Carlo simulation, where we draw 10^9 random deviates according to the above distributions:

$$x \sim \mathrm{Exp}(1.82) \quad (2)$$

$$R_{hl} \sim \mathcal{N}(1.9, 0.4^2) \quad (3)$$

$$\theta \sim \mathcal{U}(0, \pi), \quad (4)$$

where θ is the azimuthal angle around the face of the galaxy. Here we use Exp, $\mathcal{N}(\cdot)$, and $\mathcal{U}(\cdot)$ to represent exponential, normal, and uniform distributions, respectively. In Table 1, we list several other assumptions regarding the Wide-Field Instrument (WFI) and cosmological

Table 1: Basic Assumptions

Assumption	**Value**
pixel scale	$p = 0\farcs11$ pix^{-1}
dispersion	$\mathrm{d}\lambda/\mathrm{d}s = 10.8$ Å pix^{-1}
cosmology	$\Omega_0 = 0.286$
	$\Omega_\Lambda = 0.714$
	$H_0 = 69.6$ km s^{-1} Mpc^{-1}

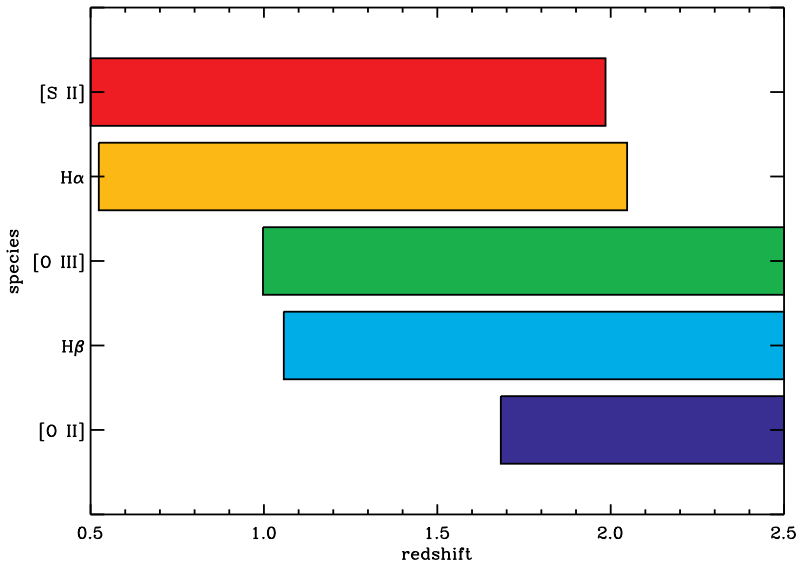

Figure 3: The redshift range for various emission lines, assuming a nominal wavelength range of 1–2 μm. The fiducial plan for the redshift survey with WFIRST uses emission lines over these redshift ranges.

model. For each random deviate, we compute the error in observer-frame redshift wavelength from the offset ELR from the galaxy center as:

$$\delta\lambda = \frac{r\cos(\theta)}{p}\,\frac{\mathrm{d}\lambda}{\mathrm{d}s}\,\frac{(1+z)^2}{d_L(z)}, \tag{5}$$

where $d_L(z)$ is the luminosity distance. We compute the expected redshift accuracy as

$$\frac{\delta z}{1+z} = \frac{1}{1+z}\frac{\delta\lambda}{\lambda}. \tag{6}$$

As indicated in Figure 3, we consider five common emission lines and a nominal wavelength range of 1–2 μm. For each possible spectral feature, we draw 10^9 deviates from Equation 2, and we show the root-mean-square (RMS) for $\delta z/(1+z)$ as a function of redshift in Figure 4.

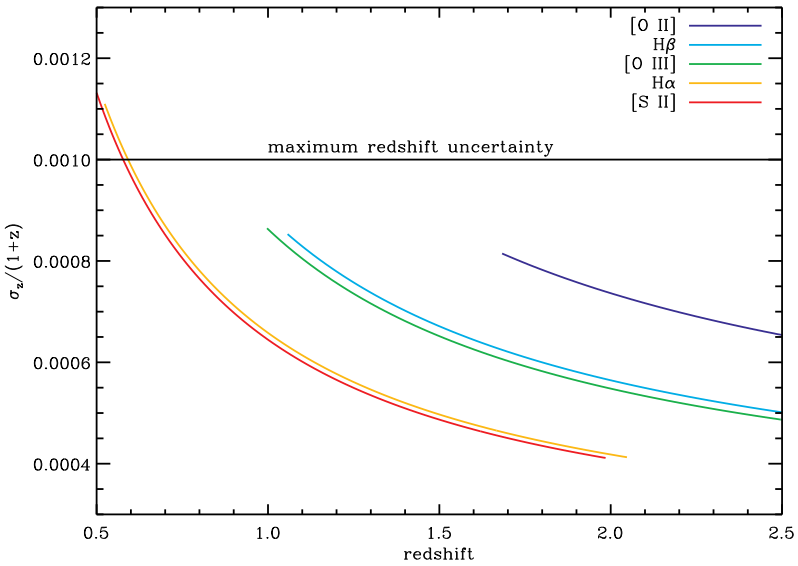

Figure 4: Estimated redshift accuracy for various emission lines (the colors have the same meaning as Figure 3). Each line represents the RMS of 10^9 deviates of Equation 6 with points drawn the distributions in Equation 2. For most redshifts and emission lines, the typical redshift uncertainty is just slightly below the WFIRST requirement (horizontal black line). Therefore we discuss three mitigation options based on instrument design, observing strategy, and data analysis in § 3.

3 Discussion

The WFIRST-AFTA Final Report requires a redshift accuracy of $\sigma_z/(1+z) \leq 0.001 - 0.005$ (Spergel *et al.* 2015) for various tests of cosmic expansion history and structure growth (weak lensing, baryon-acoustic oscillations, and supernovae light curves). Using a simple Monte Carlo simulation we have demonstrated that the typical size of galaxies at $z \sim 1$ may result in redshift errors comparable to this requirement, which suggests the need for additional corrections. This error could be mitigated in a number of ways, including instrument design, observing strategy, and data analysis. Since the wavelength uncertainty depends on several instrument properties (see equation 5), the instrument design could be tuned to minimize this effect. The parameters of the WFI grism are under active discussion, and may result in a higher dispersion than assumed in the Design Reference Mission (DRM) — thus a smaller redshift error induced by spectral diversity. This *fine-tuning* option seems the least desirable as several distinct experiments have constraints on the properties of the WFI, and what possible negative effects such changes will have on these goals should be considered more carefully.

Observing strategy could be a powerful tool to mitigate the impact of spectral diversity through observations at multiple roll angles or dispersion directions. One extreme example would be taking observations in exactly opposite position angles, resulting in a 180° difference. In principle, such observations will suffer exactly opposite wavelength errors, as the displacement between the continuum and the line emission will project with opposite sign onto the wavelength axis. The simplest approach might then be to average the observer-

frame wavelengths of emission lines to *null out* this effect. In practice, the 180°-flip approach must be verified with detailed simulations, since any contamination from neighboring objects will affect the image pairs and the role of image distortion may complicate the naïve averaging process.

Analysis with tailored observation strategy is probably the most viable approach to mitigating the spectral diversity issue. It may be possible to constrain the location of line-emitting regions, as opposed to continuum emission, either from broadband colors or by taking advantage of dispersed observations obtained at different orientations. The use of broadband colors to select subregions within a galaxy that are likely to emit spectral lines is not yet fully understood, and will likely require new extraction techniques. Software that can take advantage of the additional spatial information from multi-roll angle data is being developed to analyze HST/WFC3 data (*e.g.* Ryan *et al.* 2016), and provide the ability for efficient dispersed-image simulation, which facilitates non-linear model-fitting of dispersed data (*e.g.* Brammer *et al.* 2016).

On the other hand, Straughn *et al.* (2008) demonstrate the ability of *triangulation* to hone in on the position of the line emission (see also Figure 1). Pirzkal *et al.* (2016) extend this philosophy to identify possible *naked emission lines* (emission lines identified solely in the dispersed image without an obvious source in the direct imaging). The triangulation approaches have the advantage of not explicitly requiring broadband imaging, however this comes at tremendous computational expense and limits the overall depth to which lines can be recovered (*i.e.* the emission lines must be detected in the two-dimensional spectra of a single-orient exposure or combination).

4 Conclusion

As mentioned above, the WFIRST-AFTA Final Report (Spergel *et al.* 2015) requires fairly accurate redshifts ($\sigma_z/(1+z) \lesssim 0.001$) over $\gtrsim 2000$ deg^2 to conduct the tests on cosmological expansion. However the galaxies that offer the most promise in satisfying these requirements are known to have clumpy emission-line regions. We have demonstrated that spatial offset of the emission-line regions leads to an error in observer-frame wavelength, which translates to an additional redshift uncertainty. Depending on various assumptions, this uncertainty is comparable to the WFIRST-AFTA Final Report requirement, therefore we conclude that this geometric effect, and possible mitigation strategies, warrants further investigation.

5 Acknowledgements

We would like to thank members of the Slitless-Spectroscopy Working Group at STScI for their numerous helpful discussions. This work was carried out at Space Telescope Science Institute (STScI) under contract with the WFIRST Project Office at NASA Goddard Space Flight Center (GSFC), in the context of the WFIRST Science Operations Center, which is a partnership between GSFC, STScI, and the Infrared Processing and Analysis Center (IPAC).

6 References

Brammer, G. B., *et al.* 2016, in prep

Ferguson, H. C., *et al.* 2004, ApJL, 600, L107

Guo, Y., *et al.* 2015, ApJ, 800, 39

Law, D. R., Steidel, C. C., Shapley, A. E., Nagy, S. R., Reddy, N. A., & Erb, D. K. 2012, ApJ, 745, 85

Nelson, E. N., *et al.* 2012, ApJ, 747, L28

Mosleh, M., *et al.* 2012, ApJL, 756, L12

Nagy, S. R., *et al.* 2011, ApJ, 735, L19

Pirzkal, N., *et al.* 2013, ApJ, 772, 48

Pirzkal, N., *et al.* 2016, in prep

Ravindranath, S., *et al.* 2006, ApJ, 652, 963

Ryan, R. E., *et al.* 2016, in prep

Spergel, D., *et al.* 2015, arXiv: 1503.03757

Straughn, A. N., *et al.* 2008, AJ, 135, 1624